OPTOELECTRONICS AND ADVANCED MATERIALS – RAPID COMMUNICATIONS Vol. 4, No. 9, September 2010, p. 1391 - 1395

Interlaminar fracture properties of glass fiber reinforced poly (urethane-isocyanurate) composites prepared by SRIM process

TANG HONGYAN
Key laboratory of Advanced Textile Materials and Manufacturing Technology, Ministry of Education, Zhejiang Sci-Tech University, Hangzhou 310018, China

Poly(urethane-isocyanurate)(PUI) resin and glass fiber continuous strand mat reinforced PUI composites(CSM/PUI composites) were prepared by structural reaction injection molding process. Mode Ⅰ interlaminar fracture behaviors by use of double cantilever beam (DCB) tests were studied. It showed G_{Ic} varied significantly during crack propagation. G_{Ic} of CSM/PUI composites were higher than that of the pure PUI resin because of the additional force required to fracture fiber bridging in CSM/PUI composites. Comparative DCB tests were carried out to demonstrate the occurrence of fiber bridging. G_{Ic} varied markedly and were much dispersed, which would induce little variation when initial crack length was 40 mm. The fracture characteristics were analyzed by scanning electron microscope.

(Received August 2, 2010; accepted September 15, 2010)

Keywords: Poly(urethane-isocyanurate), Structural reaction injection molding(SRIM), Micro-phase separation, Interlaminar fracture toughness

1. Introduction

Structural reaction injection molding (SRIM) is a process for the high speed production of complex structural composites parts by placing a fiber preform in the mould cavity. Polyurethane is a main resin in SRIM process and widely applied. However, the parts made of polyurethane can normally be used at about 80 ^{o}C and may distort when long used at a higher temperature. It can significantly improve heat-resistance of polyurethane when polyisocyanurate is incorporated to form PUI by means of copolymerization [1, 2]. A delamination is one of the main damage modes of two-dimensional fabrics reinforced structural composites parts [3-5]. In fact, a delamination is the result of interlaminar crack propagation. The interlaminar fracture toughness becomes one of the important indexes of the properties for the matrix [6-9]. In general, a delamination within a composite structure would be subjected to a mixture of mode I (opening), mode II (forward shear), mode III (anti-plane shear) crack driving forces [4,6,10]. It is more appropriate that interlaminar fracture toughness of the composites is described by critical energy release rate G_{Ic}, G_{IIc} and G_{IIIc} [4,6,10]. Mode Ⅰ delamination is the lowest fracture energy mode, consequently most attention has been focused on assessing mode Ⅰ delamination propagation as a measure of the damage tolerance of structural polymer composites parts. Previous literature showed characterization of mode Ⅰ and Ⅱ interlaminar fracture behaviors was developed using carbon fiber reinforced high performance matrixes such as epoxy resins or polyetheretherketone (PEEK) [11-17]. Consequently, these testing protocols had been predominantly applied to the study of carbon fiber based materials. There were few investigations of the interlaminar fracture behaviors of other thermosetting composites which were reinforced by glass fiber. Until now, there are no studies on the interlaminar fracture behaviors of glass fiber mat reinforced PUI composites prepared by SRIM process.

In this paper, the pure PUI resin and CSM/PUI composites were prepared by SRIM process. Mode I interlaminar fracture behaviors of the pure PUI resin and CSM/PUI composites by use of double cantilever beam (DCB) tests were studied and compared with that of a standard, unidirectional carbon fiber reinforced epoxy composite(CF/EP composites) [18,19]. The fracture area along crack propagation was analyzed by SEM to identify the fracture characteristics.

2. Experimental

2.1 Materials

The isocyanate was uretonimine modified 4,4'-diphenylmethane diisocyanate (MDI-100LL) with NCO(%Wt)=28~30, the viscosity（25℃）≤60mPa•s, supplied by Yantai Wanhua Polyurethane Company (Yantai, China). The polyether polyols were GE-220A and GEP-330N supplied by Shanghai Gaoqiao Petrochemical Company (Shanghai, China), with hydroxyl values of 54~58 mg KOH/g and 33.5 ～ 36.5 mg KOH/g, respectively and percent of water containing less than 0.05%. The catalysts were DabcoTMR-3 and DabcoT12, supplied by Air Products Company (US). The catalyst content was defined as the weight percent relative to the polyether polyol weight used. Glass fiber continuous

strand mat (CSM) and unidirectional continuous fiber with nominal density of 300g/m^2 are supplied by Nanjing fiberglass Research & Design Institute (Nanjing, China).

2.2 Preparation of the pure PUI resin and CSM/PUI composites

The pure PUI resin was formed from two liquid reactants: The isocyanate (MDI-100LL) and the polyols (GE-220A and GEP-330N) the catalysts DabcoTMR-3 and DabcoT12. Initial reactant temperatures were 35 °C and 50 °C, respectively. The dimensions of the rectangular mold cavity were 350×220×5 mm^3, within which were tubes for water to keep the mold at 80 °C. After a mold release agent was applied to the entire mold surface, CSM were placed in the mould cavity. The mats were cut to give a tight fit against the side walls. Finally the liquid reactants mixture was injected into the mold by a Gusmer RIM machine, cured and then CSM/PUI composites were produced. When no CSM were placed in the mould cavity, the liquid reactants mixture was injected into the empty mold, cured and the pure PUI resin was produced.

2.3 Mode I interlaminar fracture test

Mode Ⅰ interlaminar fracture tests were carried out at 22℃ according as ISO 15024 [19]. Force-displacement data were obtained using an Instron Universal Testing Machine operating at a crosshead speed of 3.0 mm·min^{-1}. Dimensions of a DCB specimen for glass fiber based composites were shown in Fig. 1. A Polytetrafluoroethylene (PTFE) film of thickness 13 μm was inserted in the central layer at one end of the test specimens before the process, which was employed to create a initial crack from initial load. Two aluminium blocks bonded to the specimens with epoxy adhesive were used to transfer the applied load from the machine to the DCB specimens. Observation of the crack propagation during tests was facilitated by coating edges of the specimens with white acrylic paint and placing indicator marks along the coated edges. Marks were drawn at 5 mm intervals along edges of the specimen, extending at least 60 mm beyond the tip of the insert. Additionally, the first 10 mm and last 5 mm were marked at 1 mm intervals. The interlaminar fracture toughness was evaluated using the critical energy release rate G_{Ic} by Eq.1 [19].

$$G_{Ic}=\frac{3P\delta}{2b(a+|\Delta|)}\times\frac{F}{N} \tag{1}$$

where,

P-load; δ-load line displacement; b-Specimen width; Δ-correction term;

a- total crack length ($a=a_0+\Delta a$, Δa is crack propagation length), a is measured along the curved coordinate scale fixed to the specimen, as described by Fig. 2;

F- the large-displacement correction(described by Eq.2);

N- the load block correction(described by Eq.3)

$$F=1-\frac{3}{10}(\frac{\delta}{a})^2-\frac{2}{3}(\frac{\delta\cdot l_1}{a^2}) \tag{2}$$

$$N=1-(\frac{l_2}{a})^3-\frac{9}{8}\left[1-(\frac{l_2}{a})^2\right]\frac{\delta\cdot l_1}{a^2}-\frac{9}{35}(\frac{\delta}{a})^2 \tag{3}$$

Where,

l_1 - the distance from the center of the loading pin to the midplane of the specimen; l_2 - the distance from the loading pin center to its edge of the load block

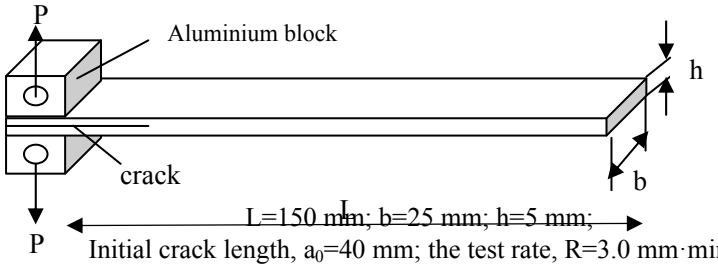

Fig. 1. Schematic diagram of a DCB specimen for mode I interlaminar fracture test.

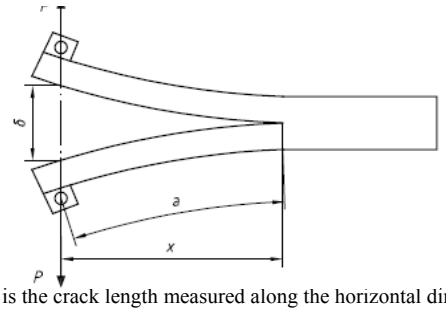

x is the crack length measured along the horizontal direction;

a is the crack length along the curved coordinate scale fixed to the specimen.

Fig. 2. The DCB specimen under the load.

3. Results and discussion

3.1 Effect of V_f (the volume of fiber) on the interlaminar fracture properties

Typical mode I interlaminar fracture data were shown in Fig. 3. Fig. 3a showed the force-displacement plots for CSM/PUI composites and CF/EP composites [17, 18]. The displacement of the CSM/PUI composite was much greater than that of CF/EP composite, which showed the high flexibility of the specimen and the need to account and correct for large displacement, F(described by Eq. 2). The force-displacement plot of CF/EP composite was linear prior to crack initiation, after which the force dropped as the crack propagates. The sudden drop in force immediately after crack propagation was typical of brittle materials. Crack propagation in this type of composite was relatively stable. In contrast, the plot of CSM/PUI composites exhibited distinct curvature prior to initiation, which occurred at a much greater displacement. Crack propagation was unstable and there was evident repeated crack initiation and crack arrest. The force-displacement plots reflected the difference in toughness of the pure PUI resin compared with that of the epoxy resin.

Mode Ⅰ force-displacement plots were used to form delamination-resistance curves(R-curves) in Fig. 3b, which showed the delamination resistance with delamination length (crack propagation length Δa). Fig. 3b showed that G_{Ic} varied significantly during crack propagation, with values lying between the upper and lower bounds with a variation in G_{Ic} of 1.0 $kJ \cdot m^{-2}$,corresponding to crack initiation and crack arrest. In contrast, the R-curve for CF/EP composite was relatively flat and a single propagation value can be obtained, which also showed crack propagation in this type of the composite was relatively stable.

Values of G_{Ic} determined from Mode I interlaminar tests were summarized in Table 1. Values of G_{Ic} for CSM/PUI composites were significantly higher than that for the pure PUI resin, which were explained by the additional force required to fracture fiber bridging in CSM/PUI composites. In contrast, CF/EP composite was produced using individually stacked plies of unidirectional CF pre-impregnated with the epoxy resin and had little interlaminar fiber bridging. Consequently, during DCB test, fiber bridging can be negligible and crack propagation along the midplane was relatively smooth.

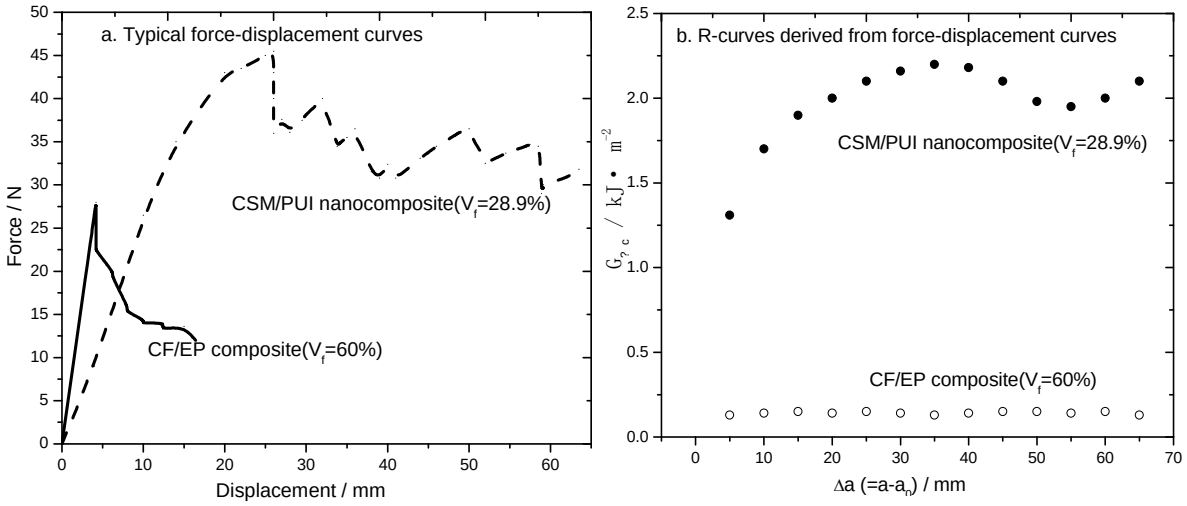

Fig. 3. Mode I interlaminar fracture behaviors of CSM/PUI composites and CF/EP composites.

Table 1. Values of G_{Ic} for the pure PUI resin, CSM/PUI composites and CF/EP composite.

Material	V_f [%]	G_{Ic} [$kJ \cdot m^{-2}$]
The pure PUI resin	0	0.6
CSM/PUI composite 1#	12.5	1.0~2.1
CSM/PUI composite 2#	21.2	1.1~2.0
CSM/PUI composite 3#	28.9	1.3~2.2
CSM/PUI composite 4#	36.7	1.4~2.3
CF/EP composite	60	0.15

To demonstrate the occurrence of fiber bridging, comparative DCB tests were carried out using a hybrid composite, in which two plies of unidirectional continuous fiber were incorporated into the central ply to displace the corresponding plies of CSM/PUI composites. The total number of glass fiber plies for the hybrid composite was the same as that for CSM/PUI composites (V_f is 28.9%). The central two unidirectional plies can significantly reduce interlaminar fiber penetration and eliminate fiber bridging during crack propagation. R-curves for CSM/PUI composites (V_f is 28.9%) and the hybrid composite were shown in Fig. 4. There was markedly less variation in G_{Ic}

with crack length for the hybrid composite, the value of G_{Ic} for the hybrid composite was about 0.7 $kJ \cdot m^{-2}$, which was similar to that of the pure PUI resin in Table 1.

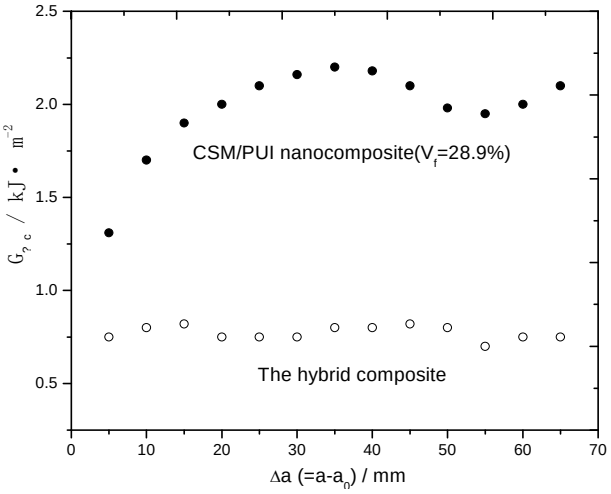

Fig. 4. Comparative R-curves for CSM/PUI composite and the hybrid composite.

3.2 Effect of initial crack length on the interlaminar fracture properties

In mode Ⅰ interlaminar fracture tests, different initial crack lengths a_0 were used in different literatures. We also found that a_0 affected values of G_{Ic} in the experiments. Fig. 5 showed effects of a_0 on values of G_{Ic}. When a_0 was 25 mm, values of G_{Ic} varied markedly and were much dispersed. As a_0 increased, the degree of dispersing was reduced. Because the inserted film would influence the resin flow and form the rich area in the resin. Values of G_{Ic} determined in this area may be invalid. Therefore, the initial crack length may not be too long. When a_0 was 40 mm, values of G_{Ic} showed little variation. Therefore, 40 mm was chosen as initial crack length in this study.

3.3 SEM photos of the fracture area

After Mode I interlaminar fracture tests, the fracture areas of CSM/PUI composites were analyzed by JEM-5610 SEM to identify the fracture characteristics. Fig. 6 were SEM photos of the fracture areas when the distance of crack propagation length $\Delta a(=a-a_0)$ was about 45 mm. It showed the surface of the fiber was not bare and clean, which indicated good interface bonding of fiber/matrix. Therefore, the crack propagation can be transferred from the matrix to the interface of fiber/matrix, and finally to the fiber through the good interface. In general, the fiber can endure high applied load, therefore the fiber based composites can achieve high mechanical properties. Cook-Gordon Damage Theory [6] mentioned values of G_{Ic} for thermosetting materials would be mainly decided by the interface of fiber/matrix. As a result, CSM/PUI composites can achieve high mechanical properties because of good interface bonding.

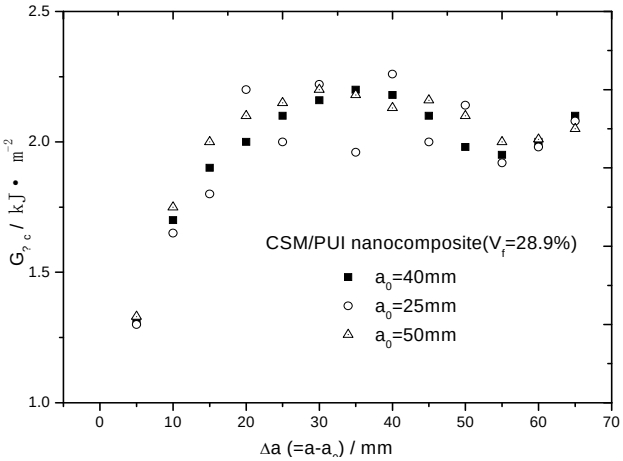

Fig. 5. Typical R-curves of different initial crack length a_0.

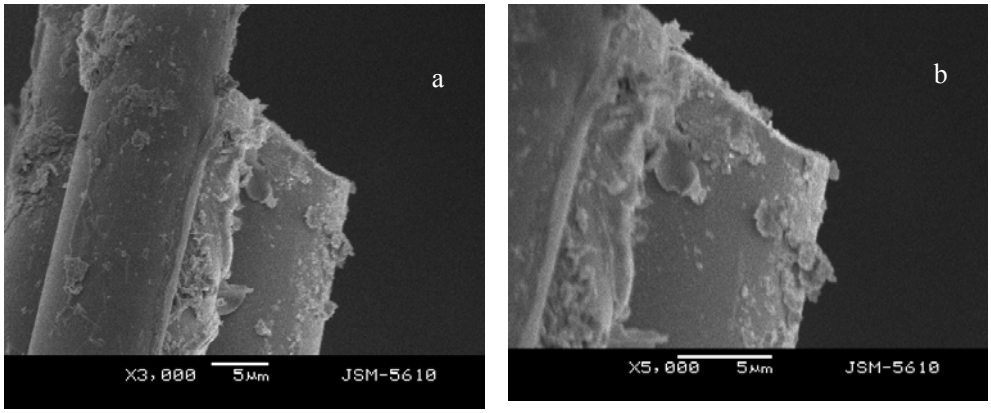

Fig. 6. SEM photos of the fracture area in the region of Δa is about 45 mm a: ×3000, b: ×5000.

4. Conclusions

The pure PUI resin and CSM/PUI composites were prepared by SRIM process. Mode I interlaminar fracture behaviors by use of double cantilever beam (DCB) tests were studied. G_{Ic} varied significantly during crack propagation. The occurrence of fiber bridging led to significant variation of G_{Ic} (1.0~2.3kJ·m^{-2}) of CSM/PUI composites and higher G_{Ic} than that of the pure PUI resin (0.6kJ·m^{-2}). When initial crack length was 40 mm, G_{Ic} showed little variation. Crack propagation can be transferred from the matrix to the interface of fiber/matrix, finally to the fiber, which indicated good interface bonding in CSM/PUI composites.

Acknowledgements

This work was supported by Science Foundation of Zhejiang Sci-Tech University (ZSTU) [Grant No. 0801605-Y].

References

[1] Zhu Lvmin, Liu Yijun: Polyurethane foam plastics (Beijing chemisty industry press, Beijing 2005).
[2] Hepburn C: Polyurethane elastomer (Ting Jiagong press, Beijing 1987).
[3] Bai Jing, Meng Qingchun and Zhang Hang: Acta materiae compositae sinica Vol. **19**, 75 (2002).
[4] O'Brien TK. ASTM STP775 (1982).
[5] Gao Feng, Jiao Guiqiong, Ning Rongchang, Journal of northwestern polytechnical university **23**, 184 (2005).
[6] O. Ishai, N. Sela, Composites **20**, 423 (1989).
[7] T. Ogata, D. Evans, A. Nyilas, Adv. Cryog. Eng. **44**, 269 (1998).
[8] Y. Shindo, R. Wang, K. Horiguchi, J. Eng. Mater. Technol. **121**, 367 (999).
[9] Y. Shindo, R. Wang, K. Horiguchi, J. Eng. Mater. Technol. **123**, 112 (2001).
[10] L. A. Carlsson, J. W. Gillespie, Application of fracture mechanics to composite materials (Elsevier, Amsterdam 1989).
[11] Wang Rui, Guo Xingfeng, Wang Guangfeng: Acta materiae compositae sinica **21**, 68 (2004).
[12] Li Yong, Li Shunlin, Tao Jie: Transactions of Nanjing University of Aeronautics and Astronautics **18**, 176 (2001).
[13] Dong Yanjin, Yang Haisheng, Bai Yilong: Chinese Journal of Materials Research **13**, 148 (1999).
[14] J. W. Gillespie, L. A. Carlsson, A. J. Smiley, Composites science and technology **28**, 1 (1987).
[15] R. H. Martin, G. B. Murri, ASTM SIP1059 (1990).
[16] P. J. Hine, B. Bew, R. A. Duckdtt, Composite science and technology **35**, 31 (1989).
[17] X. R. Xiao, J. Denault, T. Khanh, Journal of thermoplastic composite materials **5**, 64 (1992).
[19] Ciba Geigy composites technical data. Cambridgeshire: Ciba Geigy (1995).
[20] ISO 15024, Fibre-reinforced plastic composites-determination of mode I interlaminar fracture toughness, $G_{\square c}$, for unidirectionally reinforced materials.

*Corresponding author: hytang2004@163.com